

RESEARCH ARTICLE

Changsha ware glaze color: Composition, nanostructure, and copper and iron speciation

MingYue Yuan¹  | JiaYu Hou²  | XingGuo Zhang³ | Nigel Wood⁴ |
Judit Molera⁵  | Hiram Castillo-Michel⁶ | Marine Cotte^{6,7} | Trinitat Pradell¹ 

¹Physics Department and Barcelona Research Centre in Multiscale Science and Engineering, BarcelonaTech, Campus Diagonal Besòs, Universitat Politècnica de Catalunya, Barcelona, Spain

²Department of Conservation Science and Key Research, Base of Ancient Ceramics, The Palace Museum, Beijing, China

³Hunan Provincial Institute of Cultural Relics and Archaeology, Changsha, China

⁴Research Laboratory for Archaeology and the History of Art, University of Oxford, Oxford, UK

⁵MECAMAT, Facultat de Ciències Tecnologia i Enginyeries. Universitat de Vic – Universitat Central de Catalunya, Vic, Spain

⁶ESRF, The European Synchrotron, Grenoble Cedex 9, France

⁷Laboratoire d'Archéologie Moléculaire et Structurale (LAMS), CNRS, UMR 8220, Sorbonne Université, Paris, France

Correspondence

Trinitat Pradell, Physics Department and Barcelona Research Centre in Multiscale Science and Engineering, Universitat Politècnica de Catalunya, BarcelonaTech, Campus Diagonal Besòs, c) Av. Eduard Maristany 16, 08930 Barcelona, Spain.
Email: trinitat.pradell@upc.edu

Funding information

MINECO (Spain), Grant/Award Number: PID2022-137783OB-I00; Generalitat de Catalunya, Grant/Award Number: 2021 SGR 00343; ALBA synchrotron Facility, Grant/Award Number: 2020094561; MCIN/AEI, Grant/Award Number: CEX2023-001300-M

Abstract

The opacity/transparency, color, and production of designs in Changsha ware, a Tang dynasty Chinese stoneware renowned for its polychromy and pioneering high-temperature red glaze, are studied by analyzing the composition, micro/nanostructure, and copper/iron speciation. The results shed new light on some of the most debated questions about Changsha ware. In particular, the role of glaze thickness, composition, and firing conditions on the coexistence of transparent and opaque glazes and of oxidized green and reduced red copper designs on the same object, and on the reason for the development of either green or turquoise colors. New data obtained by reproducing a copper red overglaze and underglaze painting with a similar glaze composition and thickness have provided new insights into the origin of the first high-temperature copper reds and, in the absence of essential knowledge, their discontinuity. This study also contributes to the long debate regarding the use of overglaze versus underglaze painting techniques.

KEYWORDS

glaze immiscibility, glaze opacity, high-temperature copper-red, iron and copper oxidation state, overglaze versus underglaze painting

This is an open access article under the terms of the [Creative Commons Attribution-NonCommercial-NoDerivs](https://creativecommons.org/licenses/by-nc-nd/4.0/) License, which permits use and distribution in any medium, provided the original work is properly cited, the use is non-commercial and no modifications or adaptations are made.

© 2024 The Author(s). *Journal of the American Ceramic Society* published by Wiley Periodicals LLC on behalf of American Ceramic Society.

1 | INTRODUCTION

The Changsha kiln was a well-known export kiln that flourished in the late Tang Dynasty (9th–10th centuries) in southern China. The kilns were located in Tongguan Town, Changsha, Hunan Province, and archaeological excavations have shown that Changsha ware was exported to at least 20 countries and regions along the Maritime Silk Road.¹ Changsha ware was essentially a type of high-lime (CaO) glazed stoneware fired between 1100 and 1200°C,² and its porous body shows its imperfect quality compared to other kilns of the same period. However, its brilliantly colored glazes, exotic style designs, and technological innovations (transparent and opaque glazes, polychrome designs, the production of the first copper-red designs, and glazes) make it one of the more important stoneware kilns in the history of Chinese ceramics.

The Changsha kiln initially fired transparent lime glazes and only later developed polychrome and opaque lime glazes.^{1,3} Thereafter, transparent and opaque glazes coexisted. The opacity of the lime glazes is a result of light scattering by the glass immiscibility nanostructure caused by the separation of two immiscible liquids, and is associated with a lime glaze with a high SiO₂:Al₂O₃ ratio, and fired at a temperature of around 1200°C.^{4–7} The presence of glass droplets within the glaze creates a milky appearance, reminiscent of the translucency of jade. The glass-in-glass opacity of the Changsha ware followed the production of the Huai'an kiln (Fujian province), the Wuzhou kiln (Zhejiang province), and Jun ware^{4–7} (Henan province), all operating in the Tang dynasty.⁸ The beginning of the production of opaque glazes in the Changsha workshop has been related to the addition of quartz to the traditional lime glaze, and a merging of glaze technologies from southern and northern China, due to an exchange of technology between the two regions during the *An Lushan rebellion*.⁹

Polychrome Changsha wares can be divided into two categories. The first type consists of splashes of green, turquoise, brown or red, with a white opaque or yellow-brownish transparent background. A second type shows fine, intricate drawings of flowers, birds, animals, or poems, combining green and brown, red and green, and brown and turquoise designs with a transparent glaze. Some studies have shown that some of the polychrome decorations were applied overglaze (on top of the raw glaze), while others suggest underglaze application that is painted on the surface of the raw stoneware before the glaze was applied. In some cases, even in-glaze (dissolved in the central part of the glaze) has been suggested. Some examples show a thin creamy layer between the body and the glaze. This was a clay slip applied to improve the stoneware's color, which raises some doubts about

the need for opacity. As a result, there is still controversy regarding the painting technique,^{10,11} the materials used, and the origins and reasons for the various uses of transparent or opaque glazes.

Excavations of the mid to late Tang dynasty (766–907) of the Changsha kiln revealed the existence of red painted glazes, red splashed glazes, and even a few red monochrome vessels. These findings challenged the previous assumption that the Jun ware of the Song Dynasty (960–1279) was the earliest manifestation of high-temperature red glaze in China. Scientific studies focusing on the Changsha copper red designs or glazes have consistently found the presence of copper nanoparticles.¹² In fact, the ruby red color is due to the presence of a thin layer within the glaze that contains a low fraction of small (below 50 nm) metallic copper nanoparticles.^{13–15} Due to the low solubility of metallic copper, copper exists as Cu⁺ and Cu²⁺ in a silicate melt. As the ruby red color is produced by the formation of metallic copper nanoparticles, the glaze must be reduced at some point during the firing to cause Cu⁰ precipitation and to avoid the development of other copper compounds such as cuprite (Cu₂O) or the growth of large Cu⁰ particles that can impart a livery red color. It has been suggested that a reducing atmosphere at the appropriate temperature, the addition of reducing agents such as tin¹⁶ or sulfur to the glaze,¹⁷ and a low copper content, combined with mild reducing conditions, all favor the creation of the copper red effect. Some people suggest that the green color is obtained with a high copper content, while the red color is obtained with a low copper content.¹⁸ Although this may explain the coexistence of oxidized green and reduced red copper patterns in the same object, it is still not clear why this should be the case. There is also the question of whether the production of the copper red Changsha ceramics was an occasional occurrence or whether the potters of the late Tang dynasty had already mastered the technique. This is still a much-debated subject.

In order to provide some new insights into the controversies surrounding Changsha polychrome glazed wares, a selection of examples that had previously been chemically investigated⁹ were analyzed. A combination of micro-analytical techniques was used, including field emission scanning electron microscopy images of the micro- and nanostructure and micro X-ray absorption spectroscopy (XAS) analysis of copper and iron speciation in the glazes and also in the red designs. The results obtained shed new light on some of the most debated questions on Changsha ware. In particular, the work explored the presence of transparent and opaque glazes on the same vessel and the similarities and differences with contemporary productions, in particular, Jun ware glazes, the origin of the green

and turquoise colors of glazes and decorations, the nature of oxidized green and reduced red copper designs, and reason for their coexistence on the same object. Finally, underglaze and overglaze copper painted designs with similar composition and thickness to the Changsha transparent glazes have been reproduced in the laboratory to test the hypothesis regarding the red designs' origins. This new work has provided evidence for the long-running debate on the subject of overglaze versus underglaze painting at the Changsha kilns.

2 | MATERIALS AND METHODS

The selected glazes belong to a collection of pieces that have been previously studied from a chemical point of view.⁹ They show the typical transparent and opaque lime glazes of the Changsha kiln, dated to the late Tang dynasty (8th–10th centuries). CS2 was excavated from the Huangsipu site in Zhangjiagang (Suzhou, Jiangsu province), and CS7, CS8, CS10, and CS28 were excavated from the Tongguan kiln site in Changsha. CS2, CS7, and CS8 have opaque glazes, while CS10 and CS28 have transparent glazes. CS8 has a plain green glaze, CS2 and CS7 have a white glaze with green and turquoise decoration respectively, CS10 has a transparent glaze with brown and turquoise decoration, while CS28 also has a transparent glaze with a red decoration (images of all the samples are shown in Supplementary Materials, Figure S1, and in some of the Figures below).

Some copper-red and copper-green Changsha-type model ceramics were reproduced as well in the laboratory. Porcelain tiles measuring 4 cm × 4 cm were prepared. Following drying, stripes were painted on half of the surface, left to dry, and then a raw glaze with a composition similar to the transparent Changsha glaze CS28 (62.3% SiO₂, 14.1 Al₂O₃ + 1.6% K₂O + 18.5% CaO + 3.5% MgO) was applied to the entire surface. Subsequently, the raw glaze was permitted to dry, after which new stripes were painted over the glaze on the other half of the tile's surface. The tile was subsequently fired in a gas kiln at a rate of 3°C per minute for a total of 4 h, then 0.6°C/min for 3.5 h. The gas burners were then switched off, and openings were created to facilitate cooling which took approximately 12 h. The pigment utilized was a natural copper compound containing tenorite (CuO) and a small quantity of quartz, muscovite, and calcite. Further details are provided in the Supplementary Material.

Cross-sections of the samples were embedded in epoxy resin and polished with a diamond paste down to 1 μm grade. The polished sections were examined under reflected light using a Nikon Eclipse LV100D optical microscope (OM) equipped with an Infinity 1.3C camera. The sections were coated with a carbon layer (< 20 μm thick)

and were examined in a cross-beam workstation (Zeiss Neon 40), equipped with a scanning electron microscopy (SEM) GEMINI (Shottky FE) column with an attached EDS (Ultim EDS Detector, Oxford Instruments. Aztec Oxford Instruments), operated at 20 kV accelerating voltage with 1.1 nm lateral resolution, 20 nA current. The glaze microstructures were examined and recorded in the backscattered electron (BSE) mode, which allows the different phases to be distinguished on the basis of their atomic number contrast. BSE images of the microstructures were obtained at 20 kV acceleration voltage. A focus ion beam (FIB, Ga ions, 30 kV acceleration voltage) was used to polish the surface and to obtain high-resolution secondary electron images (5 kV) of the glazes' nanoparticles when they were too small to be observed directly on the mechanically polished cross-section. The volume fraction, size distribution, and mean size of the glaze nanostructure were determined using ImageJ software (<https://imagej.net/>).

The chemical composition of the glasses was measured using a JEOL JXA-8230 electron Microprobe from the Scientific and Technological Center of the University of Barcelona, equipped with five wavelength dispersive X-ray spectrometers and a probe current of 15 nA. Mineral and glass standards (Smithsonian Microbeam Standards. <http://www.nist.gov/jres>) were used for calibration and the oxygen content was calculated by stoichiometry. The analyzed sums varied between 97.0% and 100.7%.

The nature of the particles present in the red glasses was determined by micro X-Ray Diffraction (micro-XRD). The micro-XRD patterns were obtained from thin cross-sections (approximately 200 μm) cut from small fragments of the samples embedded in epoxy resin using a low-speed diamond saw. The synchrotron micro-XRD patterns were collected at the Materials Science and Powder Diffraction beamline (MSPD BL04)¹⁹ at the ALBA Synchrotron Light in transmission geometry, using a wavelength of 0.4246 Å (29.2 keV), a spot size of 20 × 20 μm², and acquisition time of 30 s and a CCD camera, SX165 detector (Rayonix, L.L.C.). The 2D images were integrated using the d2Dplot program.²⁰ The XRD data were identified using the Powder Diffraction File Database (PDF) of the International Centre for Diffraction Data.²¹

Ultraviolet-visible (UV-Vis) diffuse reflectance measurements were obtained using a double-beam spectrophotometer (Shimadzu 2700) equipped with an Ulbricht sphere detector and recorded between 200 and 800 nm, while the NIR range (800–2000 nm) was recorded using a double-beam spectrophotometer (Shimadzu 3600). Color coordinates were calculated from the diffuse reflectance spectra using the protocol developed by the *International Commission on Illumination* (CIE), CIELab (standard illuminant D65, with barium sulfate pressed powder as a white standard).

Micro-XAS data of Fe and Cu K-edge were obtained at the ID21 beamline, ESRF.²² X-rays were generated with an undulator, and their energy was adjusted with a Si (111) double-crystal monochromator. For the analysis of samples, the beam was focused to $0.3 \times 0.9 \mu\text{m}^2$ ($v \times h$) using a Kirkpatrick–Baez mirror system. The samples were mounted vertically, at an angle of 62° with respect to the incident beam. X-rays were detected using a single energy dispersive silicon drift detector (SGX, 80 mm^2) at 28° from the sample surface. XRF maps were acquired at 9.5 keV, over 2D regions in order to locate elements and identify regions of interest. The monochromator was calibrated using the first inflection point of the copper and iron metal foils (maximum of the first derivative at 8979 eV for Cu foil, 7112 eV for Fe foil) using Athena software.²³ Spectra of some reference powders (Cu_2S , CuO, Cu_2O , Fe_2O_3 , Fe_3O_4) spread on a piece of tape and covered by an ultralene foil with an unfocused beam ($0.3 \times 0.3 \text{ mm}^2$) in transmission mode were also recorded.

Copper is either dissolved in the glaze as Cu^+ and Cu^{2+} , or precipitated as Cu^0 nanoparticles; EXAFS fitting was performed using Artemis software. The spectrum is a linear combination of model compounds, each weighted by the fraction of each compound using Artemis software.²² However, the absence of any long-range order consistent with copper ions dissolved in the glass produces smooth EXAFS oscillations, making it difficult to fit more than the first shell. The first Cu–O and Cu–Cu shells were fitted using those of Cu_2O , CuO, and metallic Cu as model compounds, each weighted by a compound fraction.

The pre-edge feature of the Fe K-edge absorption is particularly sensitive to the valence state and local geometry. The weighted peak position (centroid) is known to shift to higher energies as the ferric to ferrous iron ratio increases,²⁴ and the area provides an estimate of the coordination state. The centroid can be used to calculate the oxidation state of iron in glasses.²⁵ The Fe K-edge XANES region was also fitted using a Python code⁷ developed following procedures described in the literature.^{24,26,27} Considering that the data had standard resolution ($\Delta E = 0.5 \text{ eV}$), the fitting included some restrictions, the peaks are set to Gaussian, and the positions and the width are fixed at 2.1 eV.

3 | RESULTS

3.1 | Chemical composition of the original Changsha glazes

The chemical composition of the glazes as measured by microprobe data taken from cross-sections of the glazes

TABLE 1 Microprobe chemical analysis of the glazes (wt%).

Sample	Color	Label	SiO_2	Al_2O_3	TiO_2	CaO	Na_2O	MgO	BaO	MnO	FeO	CuO	K_2O	SnO_2	SO_3	P_2O_5
CS2	White	CS2W	58.2	7.99	0.79	21.6	0.24	3.89	0.15	0.73	1.11	b.d.	2.39	b.d.	0.01	2.45
	Green	CS2G	55.4	8.99	0.74	16.5	0.22	2.86	0.13	0.54	1.11	6.34	3.08	1.23	0.03	2.02
CS7	White	CS7W	58.7	9.31	0.88	19.8	0.17	3.72	0.19	0.66	1.23	0.25	1.46	0.19	0.10	2.51
	Turquoise	CS7T	56.5	8.48	0.86	20.7	0.18	3.90	0.21	0.67	1.11	1.37	1.55	0.94	0.05	2.77
CS8	Green	CS8G	55.3	6.53	0.62	22.2	0.38	3.62	0.23	0.80	0.95	3.07	2.12	1.12	0.01	2.15
CS10	Turquoise	CS10T	57.1	8.30	0.74	18.1	0.39	3.47	0.19	0.64	1.11	4.37	2.02	1.49	0.04	1.92
	Colorless	CS10	60.2	12.9	0.86	18.2	0.15	2.25	0.12	0.50	1.57	b.d.	1.94	b.d.	b.d.	1.35
	Brown	CS10Bw	55.1	10.5	0.87	19.0	0.13	2.42	0.21	0.53	8.89	0.11	1.68	b.d.	0.02	1.51
CS28	Backside colorless	CS28B	60.8	12.6	0.79	18.4	0.14	2.40	0.06	0.47	2.05	b.d.	1.46	b.d.	b.d.	1.37
	Colorless above red	CS28T	59.4	12.3	0.86	19.8	0.24	2.19	b.d.	0.45	1.81	0.41	1.65	b.d.	0.01	1.29
	Red	CS28R	59.6	14.0	0.85	18.3	0.26	1.85	b.d.	0.37	1.99	0.43	1.99	b.d.	b.d.	0.93

Abbreviation: b.d., below detection limits.

is given in Table 1, and a summary of the properties and microstructure of the glazes is given in Table 2.

The original Changsha glazes studied are typical lime glazes (containing between 17 and 22 wt% CaO) with relatively high contents of MgO, MnO, K₂O, and all P₂O₅ associated with the use of wood ash.^{9,28} In terms of colorants, the brown glaze contains iron (8.6% FeO) and the green and turquoise glazes contain copper (1–6% CuO) and tin (0.9–1.5% SnO₂). The green/turquoise glazes contain a few hundred ppm of As and lead and a few tens of ppm of Sb, as determined by laser ablation inductively coupled plasma mass spectrometry (for details of the analytical method, see Gratuze²⁹). These indicate the probable use of a bronze alloy as the copper source. The red area of the design has a lower copper content ($\approx 0.5\%$ Cu) than the green glazes, and also shows the presence of 400 ppm Sn, and a few tens of ppm of arsenic and lead, and about 10 ppm Sb, suggesting the use of the same bronze alloy as the copper source in both the red and green glaze-colors (Table S1).

It is also worth noting that the red decoration was analyzed directly on its surface by energy dispersive X-ray fluorescence³⁰ and showed the presence of about 0.10% SO₂ in the red/green colored area, compared with only 0.02% SO₂ in the colorless lime glaze. We did not detect any sulfur in the red glaze by microprobe analysis because, as we will see later, it is not dissolved in the glaze but forms copper sulfide particles. Sulfur is also present in all the glazes, but at very low levels (around 0.02%) and not detected by energy dispersive spectroscopy analysis attached to the scanning electron microscope.

3.2 | Micro and nanostructure of the original Changsha glazes

The cross-sections of glazes show a layered microstructure (Figure 1A) formed by, on top, the glaze (a), followed by a thin glaze-ceramic interaction layer formed by a transparent layer (b) (which appears dark in the Optical Microscope image in dark field Reflection mode) richer in Al and K and poorer in Ca than the glaze, and a white opaque layer richer in Al and K and poorer in Si and Fe than the stoneware body (c). The transparent glaze layer (b) (100 μm thick) contains some calcium-rich feldspar crystals, anorthite ((Ca,Na)Si₂Al₂O₈), whereas the white opaque layer (c) (200 μm thick) is mainly crystalline and contains mullite (Al_{4.5}Si_{1.5}O_{9.75}), quartz (SiO₂), and a few anorthite crystallites (Figure 1D).

The white opaque interfacial layer (Figure 1Ac) is a fine clay slip applied to the surface, to hide the color of the stoneware. This white slip layer is not always present in the Changsha wares, but it was present in the samples examined here. The transparent interface glaze layer

(Figure 1Ab) is the result of the interaction of the lime glaze with the slip or stoneware, leading to interdiffusion of the elements and the precipitation of calcium-rich feldspars, anorthite (Figure 1D). Finally, the stoneware (Figure 1Ad) contains mullite and quartz (Figure 1D).

All the colored layers (CS2W, CS2G, CS7T, CS8G, CS10Bw, and CS10T) appear above the transparent interface glaze layer (Figure 1A,B). The brown and turquoise decorations corresponding to CS10 seem to have been applied overglaze (Figure 1B). However, the red design of CS28 appears below a thick transparent layer and this red layer contains metallic copper nanoparticles (Figure 1C,D).

The glazes with a SiO₂/Al₂O₃ ratio above 6 (CS2W, CS2G, CS7W, CS7T, CS8G, and CS10T), Table 2, show a glass immiscibility nanostructure with darker spherical droplets in a lighter matrix in SEM-BSE mode (Figure 2) and are opaque. The droplets are rich in Si and K and the matrix is richer in Ca, Mg, P, Mn, Fe, and Cu (line scan through the droplets of CS2G shown in Figure 2). The volume fraction of the droplets in all the glazes is more or less the same for all the glazes, that is, $\approx 25\%$, while the size of the droplets varies between them from ≈ 110 nm for the turquoise glazes to over ≈ 250 nm for the green glazes and ≈ 140 nm for the white glazes.

Conversely, the glazes with a low SiO₂/Al₂O₃ ratio do not show this separated glaze nanostructure, and are transparent, Table 2. The exception is the red area of the red glaze CS28 which is also opaque, but in this case, the opacity comes from a large amount of metallic copper nanoparticles, which scatter light, and not because of the presence of a glass immiscibility nanostructure.

The interaction of the glaze (SiO₂/Al₂O₃ ratio above 6) with the slip (SiO₂/Al₂O₃ ≈ 1 –2) or stoneware (SiO₂/Al₂O₃ ≈ 3 –4) increases the aluminum content of the glaze at the interface (diffusion of Al and K from the stoneware toward the glaze and Ca and Mg from the glaze toward the stoneware), reducing the SiO₂/Al₂O₃ ratio (Table 2 and Figure 1A) and, is, therefore, responsible for the development of the droplet-free transparent glaze at the interface (transparent interface layer).

The glazes also show crystalline precipitates, the areas of the white glaze CS2W and the red area CS28R studied show the presence of Ca₅(PO₄)₃F (fluorapatite) (Figure S2A and Figure 3D), fluorapatite is by far the most common species in the apatite group and is often found in small amounts in igneous rocks. The green and turquoise glazes show SnO₂ (cassiterite) and CaSnSiO₅ (malayaite), Figure S2B (Supplementary Material), both associated with the presence of tin in the copper-containing glazes. Malayaite precipitates have been documented in calcium-rich areas of the glazes, often associated with copper-green and blue glazes.³¹ They scatter light, thereby contributing to the opacity of the glazes although the effect is minimal.

TABLE 2 Summary of the glaze characteristics.

Sample	Color	Label/opacity	Thickness (μm)	$\text{SiO}_2/\text{Al}_2\text{O}_3$ (wt%)	Glaze immiscibility nanostructure (Vol. frac., size)	Colorants	Crystalline particles
CS2	White	CS2W/opaque	470	7.3	23%, 140 nm	–	$\text{Ca}_5(\text{PO}_4)_3\text{F}$ (fluorapatite) ^(c,d)
	Green	CS2G/opaque	200	6.2	25%, 267 nm	Cu^{2+} (a,b)	SnO_2 (cassiterite) CaSnSiO_5 (malayaite) ^d
CS7	White	CS7W/opaque	250	6.3	21%, 120 nm	–	
	Turquoise	CS7T/opaque	250	6.6	21%, 114 nm	Cu^{2+} (a)	
CS8	Green	CS8G/opaque	260	8.5	26%, 255 nm	Cu^+ , Cu^{2+} (a,b)	
CS10	Turquoise	CS10T/opaque	200	6.9	25%, 109 nm	Cu^{2+} (a)	SnO_2 (cassiterite) CaSnSiO_5 (malayaite) ^d
	Colorless	CST10/ transparent	100	4.7	None	–	
	Brown	CST10Bw/ transparent	300	5.1	None	Fe^{3+} (a)	
CS28	Backside colorless	CS28B/transparent	30	4.8	None	–	
	Red	CS28T/ transparent	60	4.8	None	Cu^+ (b)	$\text{Cu}_2\text{S}^{\text{d}}$
		CS28R/red opaque	60	4.3	None	Cu^{e} (a,b)	$\text{Ca}_5(\text{PO}_4)_3\text{F}$ (fluorapatite) ^(c,d) $\text{Cu}_{2-x}\text{S}^{\text{c}}$, Cu^{d} ^(c,d)

Note: Data based on ^a UV-Vis and ^b XAS spectroscopy. The crystalline compounds are identified by ^c micro-XRD and ^d SEM.

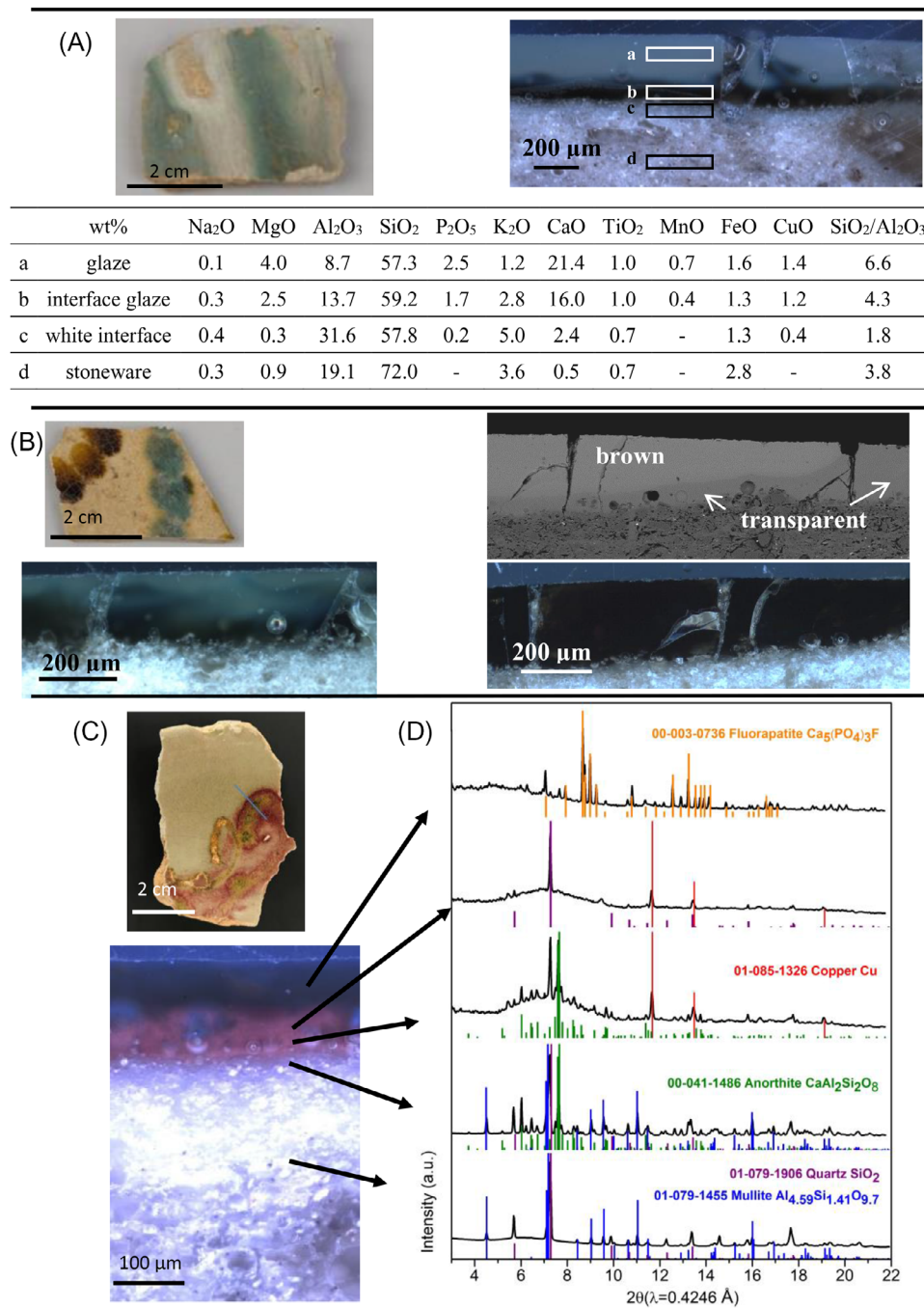


FIGURE 1 (A) Dark field Reflection OM image and SEM-EDX data obtained on different areas of CS7T, turquoise glaze, interface glaze, white interface, and body. (B) Dark field Reflection OM images of cross-sections of the turquoise (left) and brown decorations (right) of CS10 and SEM-BSD image of the same area of the brown glaze. (C) Dark field Reflection OM image of a section of the red glaze and (D) micro-XRD patterns across CS28 section. The reference PDF patterns are indicated in the figure.

The transparent upper layer of the red design (CS28T) shows the presence of some copper sulfide microcrystallites, while the red opaque layer below (CS28R) also contains a large amount of copper nanocrystallites, Figure 3B,C. Figure 4 shows some SEM-BSD images and line scans corresponding to the particles. The copper sulfide microparticles have variable copper/sulfur con-

tent, while the nanoparticles are mainly metallic copper although they are often surrounded by copper and sulfur. The composition of the larger particles mainly present in the transparent layer is close to Cu₂S, chalcocite,³² while the smaller particles mainly present in the red layer have a composition of Cu_{2-x}S with 1 < x < 2. Fluorapatite and calcium-rich feldspar crystals (anorthite),

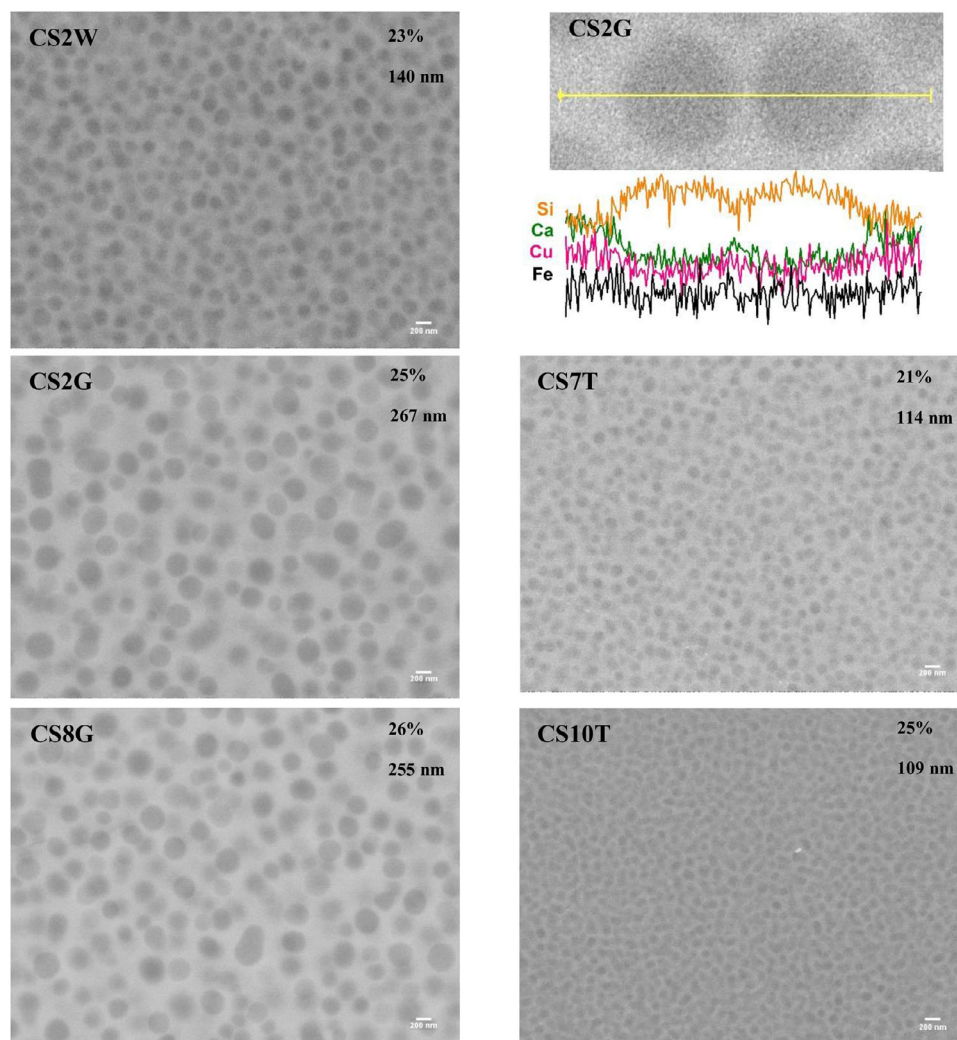


FIGURE 2 SEM-BSD images of the nanostructure of the opaque glazes showing the presence of spherical glass droplets (dark) and the glaze of the matrix (light). W (white), G (green), T (turquoise). The line scan shows that the droplets are richer in Si and poorer in Ca, Fe, and Cu than the matrix.

both surrounded by metallic copper nanoparticles, are also found at the ceramic-glaze interface in Figure 3D,E. The presence of metallic copper nanoparticles is also confirmed by micro-XRD (Figure 1D), while the copper sulfide particles are not detected. In fact, the relative scarcity and the variable composition of the copper sulfide particles together with the presence of other crystalline phases such as anorthite and fluorapatite with many reflections limit their identification.

3.3 | Colorants, transparency, and opacity: Copper and iron speciation of the original Changsha glazes

The color (colorants) and opacity of the glazes were investigated by UV-Vis-NIR spectroscopy. The white (CS2W), green (CS2G, CS8G), and turquoise (CS7T, CS10T) opaque

glazes are shown in Figure 5A, and the colorless (CS10) and brown (CS10Bw) transparent glazes in Figure 5B. The glass has a characteristic exponential decrease in absorbance (increase in reflectance) with the wavelength at which ultraviolet light is totally absorbed (Urbach edge, cutoff below 400 nm). The opaque glazes show an increase in the reflectance in the visible region (between 500 and 800 nm) due to scattering by the glass immiscibility nanostructure which is partially counteracted in the green glazes by the Cu^{2+} absorption band at 800 nm.¹³ Weak tetrahedral Fe^{3+} absorption bands between 400 and 500 nm are also visible. The white glaze also shows more clearly the broad near-infrared absorption band of Fe^{2+} in octahedral coordination at around 1100 nm.

Scattering from the glass immiscibility nanostructure is, therefore, responsible for the opacity (high reflectance in the visible) and the Cu^{2+} absorption for the green color. The size of the droplets affects the total amount of light

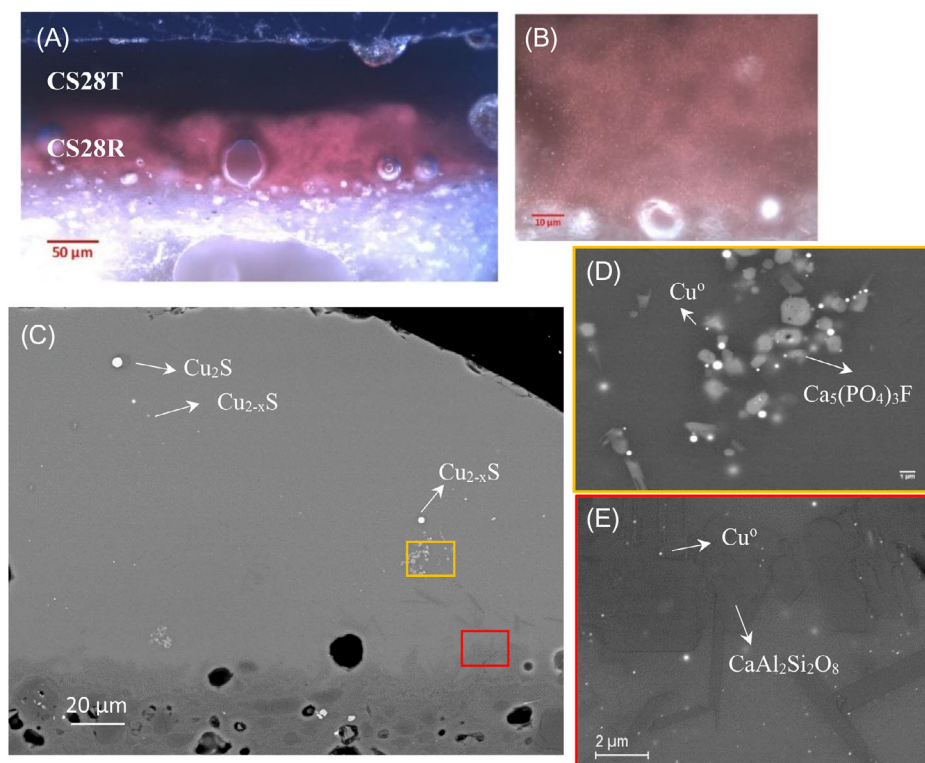


FIGURE 3 CS28 red decorated glaze. (A) Dark field OM image showing the red and colorless layers. (B) Magnification of the red area showing metallic copper nanoparticles. (C) SEM-BSD image of a cross-section of CS28 showing several crystalline precipitates. (D) Magnification of the yellow framed area showing the presence of fluorapatite crystallites surrounded by metallic copper nanocrystallites and copper sulfide microcrystallites. (E) Magnification of the red framed area showing the presence of anorthite crystals growing along the interface and metallic copper nanocrystallites.

scattered, but reducing their size also shifts the scattered light to a lower wavelength increasing the blue component. The combination of glass scattering and Cu^{2+} absorption is responsible for the final profile in the visible part of the UV-Vis spectrum and, therefore, the green color, with smaller droplets producing turquoise colors.

The transparent glazes are characterized by the absence of the scattering of the glass droplet nanostructure, Figure 5B, and also by the near-infrared absorption band of Fe^{2+} in octahedral coordination. The brown glaze shows a large absorption between 350 and 500 nm associated with tetrahedral Fe^{3+} responsible for the brown color, a faint tetrahedral Fe^{3+} band in the colorless glaze gives the glaze a yellowish color.

Figure 6B shows the UV-Vis data taken from the green and red areas of the red design of CS28, Figure 6A.³⁰ The green glaze shows the broad absorption band at 800 nm corresponding to Cu^{2+} , and the red glaze shows the surface plasmon resonance (SPR) absorption band at 560 nm associated with the presence of metallic copper nanoparticles and responsible for the red color and opacity.

The oxidation state of copper was investigated for the opaque green glaze (CS2G) and for the colorless transparent (CS28T) and red (CS28R) areas of the red decoration of

CS28 by XAS. The Cu K-edge EXAFS fitted data are shown in Table 3 and Figure S3 (Supplementary Materials). The data show that in CS2G copper is mainly present as Cu^{2+} . In the red glaze, Cu^{2+} is absent and Cu^+ is the dominant species, together with some Cu^0 , 18% Cu^0 in the red area (CS28R) and 4% Cu^0 in the colorless area (CS28T).

The oxidation state of iron was investigated for the green glaze (CS2G) and at different depths in the red glaze (CS28). Figure 7 and Table 4 show the Fe K-edge pre-edge fitted data. In detail, iron was studied near the surface of CS28TS, in the middle of the transparent area, CS28T, near the red area, CS28TR, and in the red area, CS28R, as indicated in Figure 7C.

Iron appears mainly oxidized, Fe^{3+} in the green glaze CS2G. In the case of the red design, CS28, iron is more oxidized in the colorless area near the surface (49% $\text{Fe}^{3+}/\text{Fe}_{\text{tot}}$) and becomes more reduced across the section toward the red area where iron appears completely reduced to Fe^{2+} .

In summary, in the green glaze (CS2G), both copper and iron appear mainly oxidized, whereas in the red glaze (CS28), there are two distinct areas, colorless and red, with copper and iron in the red area being more reduced than in the colorless area, and the closer to the surface the more oxidized.

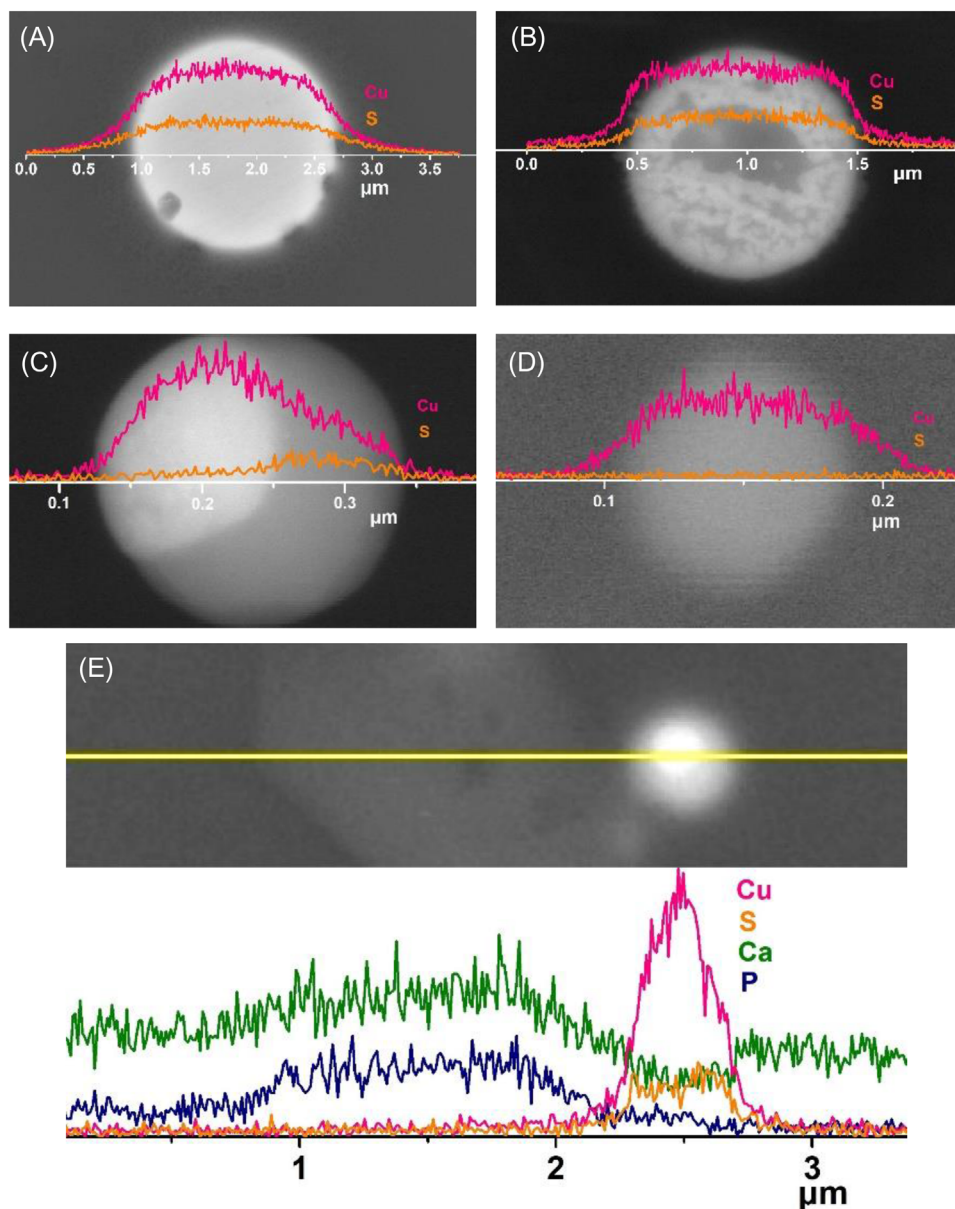


FIGURE 4 SEM-BSD and line scans of (A) copper sulfide (Cu_2S) microparticles, (B) copper sulfide microparticles with copper-rich areas, (C) partly copper sulfide partly metallic copper nanoparticles, (D) metallic copper nanoparticles, (E) metallic copper surrounded by copper sulfide nanoparticles growing near a fluorapatite microcrystal.

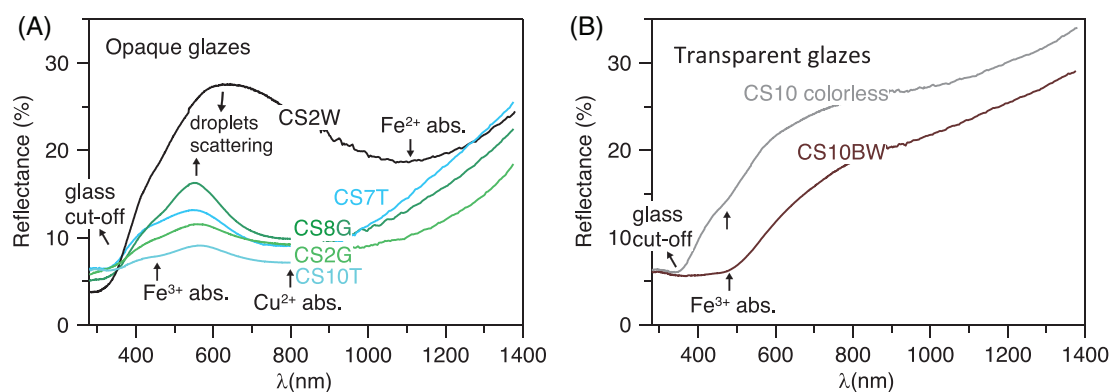


FIGURE 5 UV-Vis-NIR spectra of (A) the opaque glazes CS2, CS7, CS8, CS10T and (B) the transparent glaze CS10. W: white, T: turquoise, G: green, BW: brown. The scattering glass droplet nanostructure, the Fe²⁺, Fe³⁺, and Cu²⁺ absorption bands are shown.

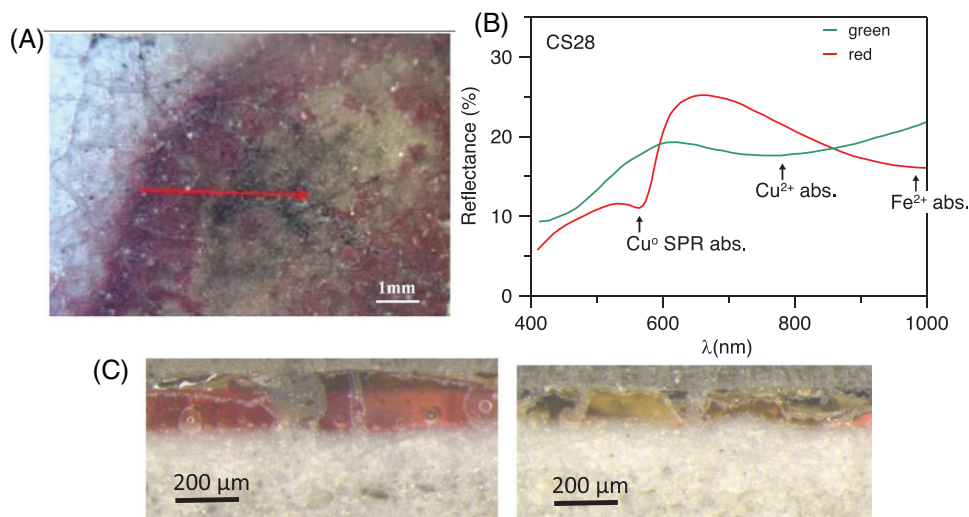


FIGURE 6 (A) Image of the red/green pattern of CS28 studied. (B) UV-Vis spectra of the green and red areas. (C) OM image of the cross-sections of the green and red areas.³⁰

TABLE 3 Cu EXAFS fitting results.

Sample	Shell	Model for fit	Model parameters	Bond length	at. fraction	R factor
			N	R(Å)	(%)	(%)
CS28R	Cu-O	Cu ₂ O	2	1.83(0)	82(2)	2.8
	Cu-Cu	CuO	12	2.52(0)	18(2)	
CS28T	Cu-O	Cu ₂ O	2	1.85*	96(4)	3.1
	Cu-Cu	Cu ⁰	12	2.55*	4(4)	
CS2G	Cu-O1	CuO	4	1.94(1)	100	1.3
	Cu-O2	CuO	2	2.76(1)		

Note: S_0^2 was fixed as 0.86. Data ranges: $3.0 \leq K \leq 9.0 \text{ Å}^{-1}$, $1.0 \leq R \leq 3.0 \text{ Å}$. The number of variable parameters is out of a total of 7.4 independent data points. The model parameters were constrained based on the crystal structure. The R-factor is a measure of the quality of the fit, lower R-factors correspond to a better fit.

*Fixed values.

TABLE 4 Fe K-edge fitting of the pre-edge peak.

	CE (eV) $\epsilon \approx 0.1$	A (eV)	Fe ³⁺ /Fe _{tot} (%) $\epsilon \approx 5\%$
CS2G	7113.5	0.20(1)	100
CS28TS	7113.2	0.22(2)	49
CS28T	7112.6	0.15(3)	20
CS28TR	7111.9	0.10(1)	0
CS28R	7112.0	0.11(1)	0

Note: Iron speciation was calculated from the CE according to Fiege et al.²⁵

Abbreviations: A, area of the peak; CE, center shift.

3.4 | Copper red/green overglaze and underglaze replicas

The cross-sections of the colored and uncolored areas of the glazes show the presence of a transparent interface glaze layer between the ceramic body and the glaze itself, formed by the interaction and diffusion of elements

from the glaze to the ceramic and from the ceramic to the glaze. This layer also dissolves the colorants (copper and iron) applied underglaze or overglaze, unless the copper is reduced to metallic nanoparticles. This layer is also thicker or thinner depending on the firing time and temperature. If the pigments are completely dissolved in the glaze, the presence of this interface layer, together with the diffusion of the colorants through the glaze makes it very difficult to determine whether the pigment has been applied overglaze or underglaze, especially if the glaze is thin. As the Changsha glazes are lime-rich ($\approx 20\% \text{CaO}$), they also provide low viscosity melts and consequently a high diffusivity of the colorants. The opaque glazes are thin compared to Jun ware glazes,⁴⁻⁷ and the transparent glazes are thinner. Pigments applied overglaze tend to produce more blurred designs than those applied underglaze, but again, this is subjective. Indeed, the brown and turquoise decoration of CS10 appears to have been applied overglaze, while the red/green decoration of CS28 seems to be applied underglaze; it is not

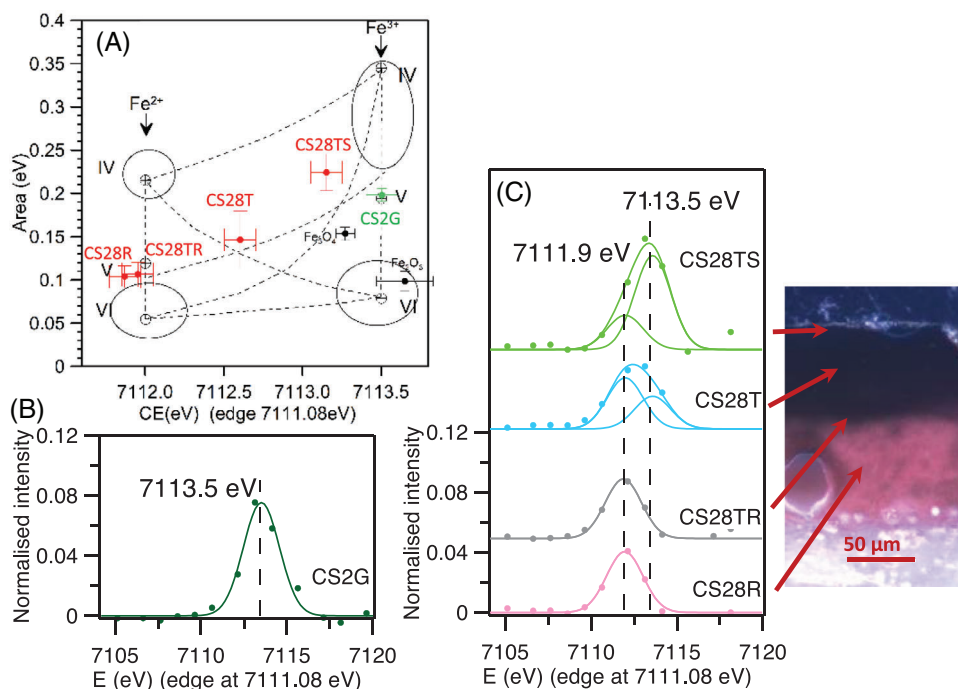


FIGURE 7 Fe K-edge XAS pre-edge peak fitting. (A) Variogram^{24–27} with data corresponding to the green glaze (CS2G) (green dots) and to measurements taken at different depths of the red glaze (CS28) (red dots) showing that iron is more oxidized near the surface and appears completely reduced in the red areas of the glaze. (B) Fitted pre-edge peak of the green glaze (CS2G) and (C) of the red glaze at different depths (CS28TS, CS28T, CS28TR, CS28R). The peak at 7111.9 eV corresponds to Fe^{2+} and at 7113.5 eV to Fe^{3+} .

clear how the decoration of CS2 was applied, perhaps overglaze.

To explore how sound these subjective judgments might be, we reproduced a copper red Changsha transparent glaze with the copper pigment applied either overglaze or underglaze to see if it was possible to distinguish between the two techniques. The ceramic was fired in a gas kiln at a high temperature under the slight reducing conditions produced by the burning of gas. Once the firing process was complete, the kiln was turned off and allowed to cool (see details in Supplementary Material). The results obtained for the copper decoration are shown in Figure 8. The color obtained is a combination of red and green, with red with some green at the edge in the underglaze paint (Figure 8B) and with red and green patches in the overglaze paint (Figure 8A). Looking at the cross-sections, in both cases, the glaze shows a two-color layer, red near the interface with the ceramic and dark greenish near the surface. The red areas contain copper nanoparticles and some a few copper sulfide particles, similar to what we found in the Changsha red glaze. Both glazes are similar in thickness (around 300 μm), except at the edge of the design where the glaze is thinner and, in this case, the color is green, although it still has some red areas/particles at the interface with the ceramic. A key finding is that it is impossible to tell from the images whether the copper pigment was applied overglaze or underglaze. The analy-

sis of the dark and red areas of the glaze in the underglaze painted pattern is shown in Table 5, and, contrary to expectation, the amount of copper is higher near the surface than near the interface. This is partly related to the interaction/dissolution of the ceramic body into the glaze. In fact, the only difference observed is the presence of very large metallic copper particles near or within the bubbles (which appear very bright in the bright field image) in the underglaze painted areas. This is not observed in the Changsha red design studied herewith.

It is also the case that it is very unlikely that overglaze and underglaze paintings were used on the same object, mainly because when the glaze mixture is applied over the underglaze colors, it forms a white deposit, and the under painted layers are no longer visible, making it extremely difficult to finish the painted design accurately with the other colors. Consequently, if both techniques were used, they were not simultaneously used in the same object.

4 | DISCUSSION

4.1 | The color and opacity of Changsha glazes and designs

We have shown that visible light scattering by the glass immiscibility nanostructure is responsible for the opacity

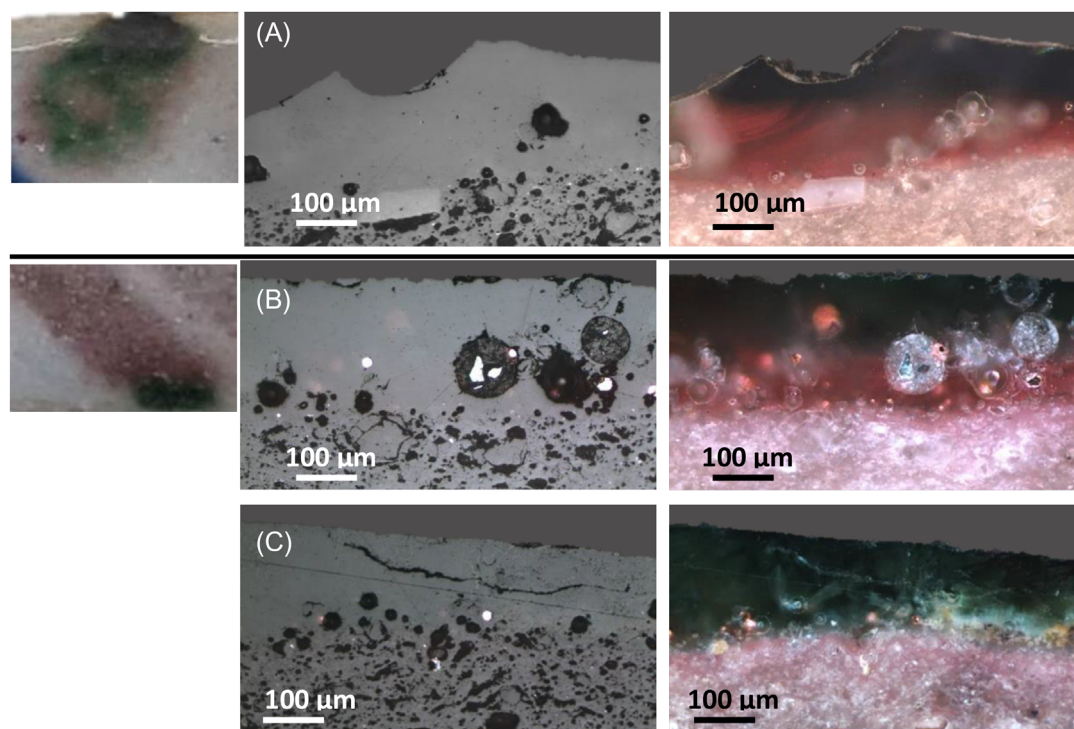


FIGURE 8 Left: Bright field and Right: Dark field optical images of a cross-section of a copper pigment fired under reducing firing and oxidizing cooling applied (A) overglaze, (B) underglaze, and (C) underglaze near the edge.

TABLE 5 SEM-EDS analysis of the underglaze painted copper design (wt%).

Underglaze painting	Na ₂ O	MgO	Al ₂ O ₃	SiO ₂	K ₂ O	CaO	TiO ₂	FeO	CuO
Dark surface area	0.1	2.8	12.9	63.3	1.4	17.7	0.1	0.6	1.1
Middle area	0.1	3.2	14.2	61.8	1.4	17.9	0.1	0.5	0.6
Red internal area	0.2	2.5	15.5	62.5	1.9	15.3	0.4	0.6	0.7

of the glazes, similar to that which occurs in Jun ware glazes.^{4,7} The droplet nanostructure results from the high Si/Al ratio in a lime glaze, which causes a Si-rich liquid and a Ca-rich liquid to separate at high temperature.⁵ The Si-rich liquid is rich in K and Na, while the Ca-rich liquid is also rich in Mg, Fe, P, Ti, and Cu if present, as in Jun glazes. The main difference is that the droplets are Si-rich and the matrix is Ca-rich, whereas in Jun glazes, it is the other way around. This is due to the high CaO content of the Changsha glazes ($\approx 20\% \text{CaO}$) compared to Jun glazes ($\approx 10\% \text{CaO}$). Consequently, the volume fraction of the calcium-rich areas in the Changsha glazes is $\approx 75\%$, whereas it is only $\approx 25\%$ in the Jun glazes. The Changsha glaze droplets are spherical and larger (between 100 and 250 nm) than the Jun glaze droplets, which are smaller (between 70 and 120 nm) and with spherical, worm-like, and may grow into largely interconnected shapes in the lime-richer glazes.⁴

Jun glazes are reduced and show creamy, millimeter-sized, calcium-rich areas (25% volume fraction of 120 nm droplets) with blue, calcium-poor areas ($< 20\%$ volume fraction of 70 nm droplets). The creamy and blue areas are the result of using a coarse-grained raw material. The opacity and light blue color result from the light scattering of calcium-rich droplets with more oxidized iron (more Fe^{3+}) giving a slight yellowish color, and in the silica-rich glass with more reduced iron (more Fe^{2+} giving the blue color).⁷ By contrast, Changsha glazes are oxidized, according to Table 4 (CS2G sample), the nanostructure is homogeneous and the calcium-rich also iron- and copper-rich areas dominate. The iron content is lower than in the Jun glazes ($\approx 1\%$ for Changsha and $\approx 2\%$ for Jun), resulting in the creamy color in the white opaque glazes.

Iron and copper are mainly reduced in the Jun glazes, $\approx 70\% \text{Fe}^{2+}$, with a broad absorption band at 1100 nm giving the glaze its characteristically blue background; copper

is mainly present as Cu^+ , which is colorless, but the presence of very few metallic copper nanoparticles gives a red tinge to the cream-colored clouds and a purple tinge to the bluish background. On the contrary, in the Changsha glazes, both copper and iron are mainly present in their most oxidized state, Cu^{2+} and Fe^{3+} . Cu^{2+} has a broad absorption band at 800 nm, which gives the glazes their characteristic green color. The larger size of the droplets affects the total amount of light scattered, increasing the opacity but also shifting the scattered light to a longer wavelength. The combination of glass scattering and Cu^{2+} absorption is responsible for the final profile in the visible part of the UV-Vis spectrum and, therefore, provides the green (large droplets) or turquoise (small droplets) colors.

The transparent glazes are characterized by a $\text{SiO}_2/\text{Al}_2\text{O}_3 < 6$, the absence of the glass droplet nanostructure scattering, and show the characteristic exponential-like absorption/reflectance of glass. The weak tetrahedral Fe^{3+} absorption band gives the colorless glaze a yellowish hue, which is also influenced by the color of the underlying stoneware surface, providing a reason to apply a white slip. The brown patterns were made with an iron-rich pigment; the high absorption between 350 and 500 nm associated with tetrahedral Fe^{3+} is responsible for the brown color.

A white slip (richer in Al and K and poorer in Si than the body) was also applied in many cases to create a smooth surface and to mask the stoneware's natural color. The interaction of the glaze with the slip increases the Al and K content at the interface, $(\text{SiO}_2/\text{Al}_2\text{O}_3)_{\text{slip}} \approx 1-2$, and, consequently, the development of a droplet-free transparent glaze. However, even in the absence of the slip, the interaction of the stoneware, $(\text{SiO}_2/\text{Al}_2\text{O}_3)_{\text{stoneware}} \approx 3-4$, with the glaze also results in an increase in the Al content at the glaze interface, although less than the slip. As a result, the thickness of the glaze layer also plays a significant role in opacity. If the glaze layer is too thin, the diffusion of Al from the slip or stoneware will result in a reduced Si/Al ratio within the glaze, resulting in a transparent glaze. Conversely, when the glaze layer reaches a sufficient thickness, the influence of the slip or stoneware diminishes, and the glaze is opaque. This is clearly seen in CS10 (Figure 1B), where the turquoise design (200 μm) above a relatively thin lime glaze (100 μm), and the turquoise design is opaque, while the glaze underneath and around is transparent (which appears dark in the Optical Microscope image in dark field Reflection mode).

We have seen that the Changsha glazes are applied very thinly (between 100 and 300 μm thick) contrary to Jun glazes which were applied very thickly (between 500 μm and 1–1.5 mm thick).

Consequently, Jun glazes also have a transparent interface glaze layer but, more importantly, they are always

opaque, while the thinner Changsha glazes may be transparent or opaque. The chemical composition of Changsha glazes from various Tang dynasty kilns found in the literature also shows that the Si/Al is higher in the opaque glazes than in the transparent glazes.^{8,33–35} Consequently, without knowing the thickness of the glazes, it is not possible to definitively conclude that the glaze composition was deliberately formulated to obtain either an opaque or a transparent effect or was the result of a thinner/thicker application of the glaze. It is highly possible, as has been suggested, that at some point, the $\text{SiO}_2/\text{Al}_2\text{O}_3$ ratio of the glazes was increased under the influence of northern potters in order to produce opaque glazes, in this case, transparent glazes were also obtained when the glazes were thin.⁹ This also explains the coexistence of transparent and opaque glazes on the same object.

4.2 | The red/green design

Examination of the red design of CS28 revealed the presence of metallic copper nanoparticles which have an intense SPR absorption band at 560 nm and are responsible for both the red color and the opacity of the glaze. Copper red glazes can be obtained by a low-temperature glaze reduction. A reducing gas is introduced during the cooling (below 800°C) to convert Cu^{2+} to cuprite (Cu_2O) and metallic copper.¹³ However, this process results in a more reduced glaze surface, whereas our Changsha red glaze has a more oxidized surface.

In fact, the red pattern has both green and red areas (Figure 6A), green in the center of the pattern and red at the edges. The glaze of the green area is thinner (Figure 6C) and contains much more copper (2.5% CuO) than the glaze of the red area (0.4% CuO).³⁰ The difference in the thickness between the green and red areas is due to the application of a high concentration of pigment. It is well known that a high concentration of pigment will repel the glaze, resulting in a thinner glaze which is enhanced by the very low viscosity of Changsha glaze. Copper diffuses around the painted design and, consequently, a highly concentrated pigment will end up as a thin, copper-rich glaze with thicker, copper-poor glaze edges.

The thin copper-rich center of the pattern is mainly oxidized (except for a few red spots) as shown in Figure 6B.²⁹ The thick copper-poor edge has a more oxidized surface (both copper and iron) giving a colorless layer over a red and more reduced layer, Figure 3A and Table 3. Copper is present as Cu^+ in the colorless area but also in the red area Cu^+ predominates (82% Cu^+ and 18% Cu^0 in the red zone), but the presence of metallic copper nanoparticles is responsible for the red color. Copper sulfide particles are also present in both the red and colorless areas but do

not give color to the glaze.¹⁷ (The presence of copper sulfide has also recently been determined in the copper red underglaze designs of early Ming porcelain.)³⁶

The glaze areas that have turned red are the edge areas of the design, which contain a low copper/sulfur ratio compared to the green central area of the drawing, 2.4 and 22.6, respectively.³⁰ This is in good agreement with a recent study showing that red glasses can contain a copper-to-sulfur atomic ratio between 2 and 2.5.¹⁷ When fired at high temperature (around 1100°C) in a reducing atmosphere, most of the copper is retained as copper sulfide and some precipitates as metallic copper, while iron is reduced to Fe^{2+} . If the conditions become more oxidizing, they would promote the oxidation of Fe^{2+} to Fe^{3+} and the oxidation of copper sulfide. This leads to the release of sulfur, now lost as SO_2 gas, the dissociation of copper into Cu_2O and metallic Cu, the precipitation of metallic copper nanoparticles, and some dissolution of Cu^+ in the glaze.

In a wood-burning kiln, oxidizing conditions frequently occur during cooling after a reducing firing. This final oxidation process will reoxidize the glaze, but this is a diffusion-controlled process through the glaze's surface. The oxidation will reach a certain depth depending on the cooling rate, therefore, thin glazes can often appear fully reoxidized, while thicker glazes will have a more oxidized surface layer over a more reduced layer beneath. Consequently, the thicker edges of the painted copper-rich design meet the conditions necessary for the development of copper red: reducing then oxidizing conditions and a suitable Cu/S ratio together with a much lower level of Cu, conducive to forming a copper-red underglaze layer. Conversely, the thin, copper-rich central part of the design will be completely oxidized. Painting with an overconcentrated pigment resulted in a thin design with thicker edges. The use of alternating oxidizing and reducing atmospheres during the firing is responsible for the red-edged green designs.

Consequently, the use of a concentrated pigment and reducing conditions at high temperature during the firing and oxidation during the cooling may have led to the first high-temperature copper red decorations. The lack of knowledge of the underlying mechanisms involved, the fact that Changsha wares were basically fired under oxidizing conditions, and some difficulties in controlling the process may be responsible for the eventual discontinuation of copper-red production at the Changsha kilns.

4.3 | Overglaze or underglaze painting

Changsha ware was produced for over a century, in the 9th century in the mid-to-late of the Tang dynasty. This is a

long period and the production was varied. It is worth noting that Chinese painting made significant progress during the Tang dynasty. Changsha ware is one of the first wares in which a wide range of motifs, including figures, flora, fauna, landscapes, abstract geometric patterns, and even poetry, were painted in a variety of colors. These decorative elements relied predominantly on fine line drawings to depict intricate details, complemented by the occasional use of dots and splashes for additional ornamentation. Fine painting requires a great deal of skill, but also a fine background, so detailed painting was usually done on the ceramic surface rather than on the raw glaze. It has been suggested that this was the reason for the change from overglaze to underglaze painting, and the first underglaze painting in China. However, our results have shown that it is almost impossible to verify the painting technique used by analyzing the distribution of colorants in the glaze thickness due to the diffusion of metals from the body to the glaze surface during firing. For a clearer view of this issue, it will be necessary to study underfired ceramic wasters in order to verify the painting techniques that were used at the different kilns involved.

5 | CONCLUSIONS

Changsha ware was essentially a type of Chinese Tang Dynasty stoneware with high-lime glazes that were fired between 1100 and 1200°C. Building on an earlier use of transparent glazes, the Changsha potters created opaque and transparent lime-rich glazes and also developed wares with a rich polychromy of brown, green, turquoise, and red.

Our data have shown that the occurrence of opacity is related to the development of a glass immiscibility nanostructure with Si-rich droplets ($\approx 25\%$ volume fraction) in a Ca-rich matrix due to the high $\text{SiO}_2/\text{Al}_2\text{O}_3$ ratio (≈ 6) and a $\approx 20\%$ CaO glaze content. The Changsha stoneware body, or the thin fine clay finish slip that is often present, interacts with the glaze, reducing the $\text{SiO}_2/\text{Al}_2\text{O}_3$ proportions and producing a transparent glaze at the body/glaze interface. Consequently, if the glaze layer is too thin, the whole glaze becomes transparent, whereas if it is sufficiently thick, the effect is diminished and the outer part of the glaze becomes opaque. This explains why, even when the glazes are formulated to be opaque, transparent and opaque glazes may coexist in the same object.

Green and turquoise polychromies and glazes are obtained by the presence of oxidized copper (Cu^{2+} and Cu^+). The change in color between green and turquoise is due to the presence of smaller glass droplets in the latter, ≈ 200 and ≈ 100 nm, respectively. The copper pigment contains tin, but also small amounts of zinc, antimony, and

lead, indicating that it was derived from bronze. The brown designs are made using an iron-rich pigment and the iron is dissolved in the glaze as tetrahedral Fe^{3+} .

A red pattern with the characteristic green color in the center and red edges was analyzed. A high concentration of pigment is known to repel the glaze to the edges, resulting in a thin, copper-rich glaze with thick, copper-poor glaze edges. The red edges show an outer transparent layer, where copper is mainly present as Cu^+ , and an inner red layer, where metallic copper nanoparticles are responsible for the red color. By using a reducing firing, the thin central part of the design becomes completely oxidized during the cooling, while the thicker edges have a more oxidized surface layer over a more reduced red layer underneath. This explains the coexistence of green- and red-colored areas in the same design.

The presence of a transparent glaze layer at the interface with an intermediate composition between the glaze and the stoneware, and the low thickness and the low viscosity of Changsha glazes, make it difficult to determine whether the decoration was applied underglaze or overglaze. This has led to a long discussion about the painting technique that was originally used. Our successful overglaze and underglaze reproductions of a red and green copper design have shown that the distribution of colorants within the glaze is not a reliable criterion to distinguish between these two methods.

ACKNOWLEDGMENTS

This work received financial support from MINECO (Spain) (grant PID2022-137783OB-I00), Generalitat de Catalunya (grant 2021 SGR 00343), ESRF (<https://doi.org/10.1515/ESRF-ES-879445008>), MCIN/AEI/10.13039/5011000011033 (CEX2023-001300) and ALBA synchrotron Facility (2020094561). The XAS experiments were performed at ID21 Beamline at ESRF with the collaboration of ESRF Staff. Micro-XRD experiments were performed at BL04 (MSPD) Beamline at ALBA synchrotron Facility with the collaboration of Alba Staff. We would like to thank Dr. Bernard Gratuze for the LA-ICP-MS analysis. Finally, we would like to thank Josep and Jan Madrenas for the use of their gas kiln to reproduce the copper red design.

ORCID

MingYue Yuan  <https://orcid.org/0000-0003-2158-5653>
JiaYu Hou  <https://orcid.org/0000-0002-6630-773X>
Judit Molera  <https://orcid.org/0000-0003-3116-0456>
Trinitat Pradell  <https://orcid.org/0000-0002-8720-5492>

REFERENCES

- Changsha Ware Research Group. Changsha ware (长沙窑). Forbidden City Press; 1991.
- Zhang ZG, Guo YY. A study on Changsha Tongguan coloured glaze and painted wares (长沙铜官窑色釉和彩瓷的研究). *J Jingdezhen Ceram Inst* (景德镇陶瓷学院学报). 1985;6(1):11–17. <https://doi.org/10.13957/j.cnki.tcxh.1985.01.003>
- Ye ZM. History of Chinese pottery and porcelain (中国陶瓷史). Beijing, China: SDX Joint Publishing Company; 2011.
- Kingery WD, Vandiver, PB. Song Dynasty Jun ware glazes. *Am Ceram Soc*. 1983;62(11):1269–1279, 1279–1282.
- Chiang YM, Kingery DW. Spinodal decomposition in a $\text{K}_2\text{O}-\text{Al}_2\text{O}_3-\text{CaO}-\text{SiO}_2$ glass. *Commun Am Ceram Soc*. 1983;6:C-171–C-172.
- Hou JY, Pradell T, Li Y, Miao J. Jun ware glazes: chemistry, nanostructure and optical properties. *J Eur Ceram Soc*. 2018;38:4290–302. <https://doi.org/10.1016/j.jeurceramsoc.2018.05.010>
- Yuan MY, Hou JY, Gorni G, Crespo D, Li Y, Pradell T. Jun ware glaze colours: an X-ray absorption spectroscopy study. *J Eur Ceram Soc*. 2022;42(6):3015–22. <https://doi.org/10.1016/j.jeurceramsoc.2022.02.016>
- Chen XQ, Zhang ZG, Huang RQ. Opaque glaze of the Changsha Tongguan ware—another Tang dynasty's phase separated glaze. *J Chin Ceram Soc*. 1991;19(3):234–40.
- Hou JY, Zhang XG, Wood N, Zhou R, Hu Y, Li H, et al. New insights into Changsha glaze (9–10 century) based on chemical composition and strontium isotope ratio. *J Archaeol Sci: Rep*. 2022;43:103455. <https://doi.org/10.1016/j.jasrep.2022.103455>
- Sun Y, Mao ZW, Zhou SR, Wang CS, Dong JQ, Yuan CX et al. Linear-scanning analysis of the coloured drawing craft of Changsha-kiln porcelain by EDXRF probe (能量色散X射线荧光光谱法探针线扫描分析“长沙窑”彩绘工艺). *PTCA (Part B: Chem Anal)* (理化分析-化学分册). 2008;44(9):807–14.
- Zhang XG, Jiang XCY, Cui JF, Lyu HS, Qiu Y. Detection and analysis of high-temperature glazed colored porcelain in Changsha kiln (长沙窑高温釉上彩瓷的检测分析). *Palace Museum J* (故宫博物院院刊). 2020;5:071–085.
- Li YQ, Yang YM, Zhu J, Zhang X, Jiang S, Zhang Z, et al. Colour-generating mechanism of copper-red porcelain from Changsha Kiln (A.D. 7th–10th century). *China Ceram Int*. 2016;42:8495–500. <https://doi.org/10.1016/j.ceramint.2016.02.07>
- Weyl WA. Coloured glasses. Sheffield: Society of Glass Technology; 1951. Reprint 2016.
- Pradell T. Lustre and nanostructures—ancient technologies revisited. In: Dillmann P, Bellot-Gurlet L, Nenner I, editors. Nanoscience and cultural heritage. Paris: Atlantis Press, 2019; p. 3–39. https://doi.org/10.2991/978-94-6239-198-7_1
- Li G, Lei Y. The computational simulation of the reflection spectra of copper red glaze. *AIP Adv*. 2022;12(9):095319. <https://doi.org/10.1063/5.0095570>
- Yuan MY, Bonet J, Castillo-Michel H, Cotte M, Schibille N, Gratuze B, et al. The role of tin and iron in the production of copper red glass. *Bol Soc Esp Cerám Vidr*. 2023;63(2):125–34. <https://doi.org/10.1016/j.bsecev.2023.07.005>
- Yuan MY, Bonet J, Cotte M, Schibille N, Gratuze B, Pradell T. The role of sulphur in the early production of copper red stained glass. *Ceram Int*. 2023;49(11)part B: 18602–13. <https://doi.org/10.1016/j.ceramint.2023.02.236>
- Zhu CX, Wang YB, Lu Q, Zhao H, Zhu X, Fa W, et al. Reproduction of Jun-red glazes with nano-sized copper oxide. *J Am Ceram Soc*. 2017;100(10):4562–69. <https://doi.org/10.1111/jace.14989>

19. Fauth F, Peral I, Popescu C, Knapp M. The new material science powder diffraction beamline at ALBA synchrotron. *Powder Diffr.* 2013;28(S2):S360–70. <https://doi.org/10.1017/S0885715613000900>
20. Vallcorba O, Rius J. d2Dplot: 2D X-ray diffraction data processing and analysis for through-the-substrate microdiffraction. *J Appl Crystallogr.* 2019;52:478–84. <https://doi.org/10.1107/S160057671900219X>
21. ICDD. Web site of the International Centre for Diffraction Data. <https://www.icdd.com/>. Accessed July 2023
22. Cotte M, Pouyet E, Salomé M, Rivard C, De Nolf W, Castillo-Michel H, et al. The ID21 X-ray and infrared microscopy beamline at the ESRF: status and recent applications to artistic materials. *J Anal At Spectrom.* 2017;32:477–93. <https://doi.org/10.1039/C6JA00356G>
23. Ravel B, Newville M. ATHENA, ARTEMIS, HEPHAESTUS: data analysis for X-ray absorption spectroscopy using IFEFIT. *J Synchrotron Rad.* 2005;12:537–41. <https://doi.org/10.1107/S0909049505012719>
24. Wilke M, Farges F, Petit PE, E Brown G, Martin F. Oxidation state and coordination of Fe in minerals: an Fe K-XANES spectroscopic study. *Am Mineral.* 2001;86(5):714–30. <https://doi.org/10.2138/am-2001-5-612>
25. Fiege A, Ruprecht P, Simon AC, S Bell A, Göttlicher J, Newville M, et al. Calibration of Fe XANES for high precision determination of Fe oxidation state in glasses: comparison of new and existing results obtained at different synchrotron radiation sources. *Am Mineral.* 2017;102:369–80. <https://doi.org/10.2138/am-2017-E102410>
26. Wilke M, Partzsch GM, Bernhardt R, Lattard D. Determination of the iron oxidation state in basaltic glasses using XANES at the K-edge. *Chem Geol.* 2005;220:143–61. <https://doi.org/10.1016/j.chemgeo.2005.03.004>
27. Boubnov A, Lichtenberg H, Mangold S, Dierk Grunwaldt J. Identification of the iron oxidation state and coordination geometry in iron oxide- and zeolite-based catalysts using pre-edge XAS analysis. *J Synchrotron Rad.* 2015;22:410–26. <https://doi.org/10.1107/S1600577514025880>
28. Wood N. Chinese glazes: their origins, chemistry and recreation. London: A&C Black; 1999.
29. Gratuze B. Glass characterization using laserablation-inductively coupled plasma-mass spectrometry methods. In: Dussubieux L, Golitko M, Gratuze B, editors. Recent advances in laser ablation ICP-MS in archaeology. Natural Sciences in Archaeology. Berlin Heidelberg: Springer Verlag; 2016; p. 179–96. <https://doi.org/10.1007/978-3-662-49894-1>
30. Jiayu H, Cui J, Xingguo Z, He L, Gen L, Hanwen L, et al. The birth of copper-red glaze: optical property and firing technology of the glaze from Changsha Kiln (8th–9th century). *J Europ Ceram Soc.* 2022;42:1141–48. <https://doi.org/10.1016/j.jeurceramsoc.2021.11.002>
31. Coentro S, Trindade RAA, Mirão J, Candeias A, C Alves L, M C Silva R, et al. Hispano-Moresque ceramic tiles from the Monastery of Santa Clara-a-Velha (Coimbra, Portugal). *J Archaeol Sci.* 2014;41:21–28. <https://doi.org/10.1016/j.jas.2013.07.031>
32. Beauvoit E, Bouquillon A, Majérus O, Caurant D, Cuny J, Thomas A. Comparative study of architectural bricks from Khorsabad and Susa sites: characterization of black glazes. *Heritage.* 2023;6:6291–310. <https://doi.org/10.3390/heritage6090329>
33. Chen YC, Jin BD. A preliminary study of Ou kiln brown coloured celadon (甌窑褐彩青瓷的初步研究). *Relics from Jiangxi (江西文物)*. 1991;4:37–40.
34. Chen XQ, Huang RQ, Chen SP. Phase-separation glazed porcelain in the 6th century A.D.— a study on Huaian ware of the Liang and the Tang dynasty. *J Chin Ceram Soc.* 1986;14(2):147–52.
35. Li WD, Li JZ, Wu J, Guo J. Study on the phase-separated opaque glaze in ancient China from Qionglai kiln. *Ceram Int.* 2003;29:933–37. [https://doi.org/10.1016/S0272-8842\(03\)00048-8](https://doi.org/10.1016/S0272-8842(03)00048-8)
36. Jia C, Li G, Guan M, Zhao J, Zheng Y, Wang G, et al. A short but glorious porcelain glaze of Early Ming Dynasty: new finding of raw material and colorants in the copper red glaze. *J Europ Ceram Soc.* 2021;41:3809–15. <https://doi.org/10.1016/j.jeurceramsoc.2021.01.018>

SUPPORTING INFORMATION

Additional supporting information can be found online in the Supporting Information section at the end of this article.

How to cite this article: Yuan MY, Hou JY, Zhang XG, Wood N, Molera J, Castillo-Michel H, et al. Changsha ware glaze color: Composition, nanostructure, and copper and iron speciation. *J Am Ceram Soc.* 2024;1–17. <https://doi.org/10.1111/jace.20025>